Since January 2020 Elsevier has created a COVID-19 resource centre with free information in English and Mandarin on the novel coronavirus COVID-19. The COVID-19 resource centre is hosted on Elsevier Connect, the company's public news and information website.

Matter

CellPress

Review

Whispering-Gallery Sensors

Xuefeng Jiang,[1] Abraham J. Qavi,[1] Steven H. Huang,[1,2] and Lan Yang[1,*]

SUMMARY

Optical whispering-gallery mode (WGM) microresonators, confining resonant photons in a microscale volume for long periods of time, strongly enhance light-matter interactions, making them an ideal platform for photonic sensors. One of the features of WGM sensors is their capability to respond to environmental perturbations that influence the optical mode distribution. The exceptional sensitivity of WGM devices, coupled with the diversity in their structures and the ease of integration with existing infrastructures, such as conventional chip-based technologies, has catalyzed the development of WGM sensors for a broad range of analytes. WGM sensors have been developed for multiplexed detection of clinically relevant biomolecules while also being adapted for the analysis of single-protein interactions. They have been used for the detection of materials in different phases and forms, including gases, liquids, and chemicals. Furthermore, WGM sensors have been used for a wide variety of field-based sensing applications, including electric field, magnetic field, force, pressure, and temperature. WGM sensors hold great potential for applications in life and environmental sciences. They are expected to meet the ever-increasing demand in sensor networks, the Internet of Things, and real-time health monitoring. Here we review the mechanisms, structures, parameters, and recent advances of WGM microsensors and discuss the future of this exciting research field.

INTRODUCTION

Our ability to understand and decipher the natural world fundamentally rests on sensors. Initially, people used their sense of sight, hearing, touch, taste, and smell to probe the natural world. Over time, a plethora of scientific instruments, such as microscopes, and eventually more sophisticated techniques such as scanning electron microscopy (SEM), replaced our natural senses to characterize the world around us. A prominent example is optical sensors, which we rely on to facilitate our everyday lives by monitoring the intensity, phase, polarization, frequency, or the speed of light. One class of optical sensors that has attracted intense attention is whispering-gallery mode (WGM) devices,[1–3] which are named after a phenomenon found in St. Paul's Cathedral in London. Within the cathedral, whispers can be heard along the curved wall of the dome because sound waves experience consecutive reflections from the circular wall of the gallery. Analogous to the propagation of sound in St. Paul's Cathedral, optical WGM resonators confine light within small structures through total internal reflection, with resonant light circulating in the structures millions of times.

Optical WGM microresonators offer inherent advantages as sensing devices. Compared with interferometric sensors, WGM sensors have the interferometric arm "folded" into its roundtrip pass, resulting in a much smaller device footprint. In addition, due to light making many round-trips in the same mode volume,

Progress and Potential

As a sensing platform that strongly enhances light-matter interactions, whispering-gallery mode (WGM) microresonators have been used for the detection of not only physical matters, such as nanoparticles, small bio/chemical molecules, or gases, but also physical parameters or fields surrounding the resonator that influence the optical modes, for example temperature, pressure, force, electric field, and magnetic field. During the last two decades, a variety of sensing mechanisms and enhancement techniques has been developed for WGM sensors. The future research efforts of WGM sensors will find numerous opportunities in life, health, and environmental sciences and are expected to meet the ever-increasing demand in sensor networks, the Internet of Things, and real-time health monitoring. Moreover, the developments of novel cavity structures and sensing enhancement mechanisms or techniques are always one of the research focuses in this area.

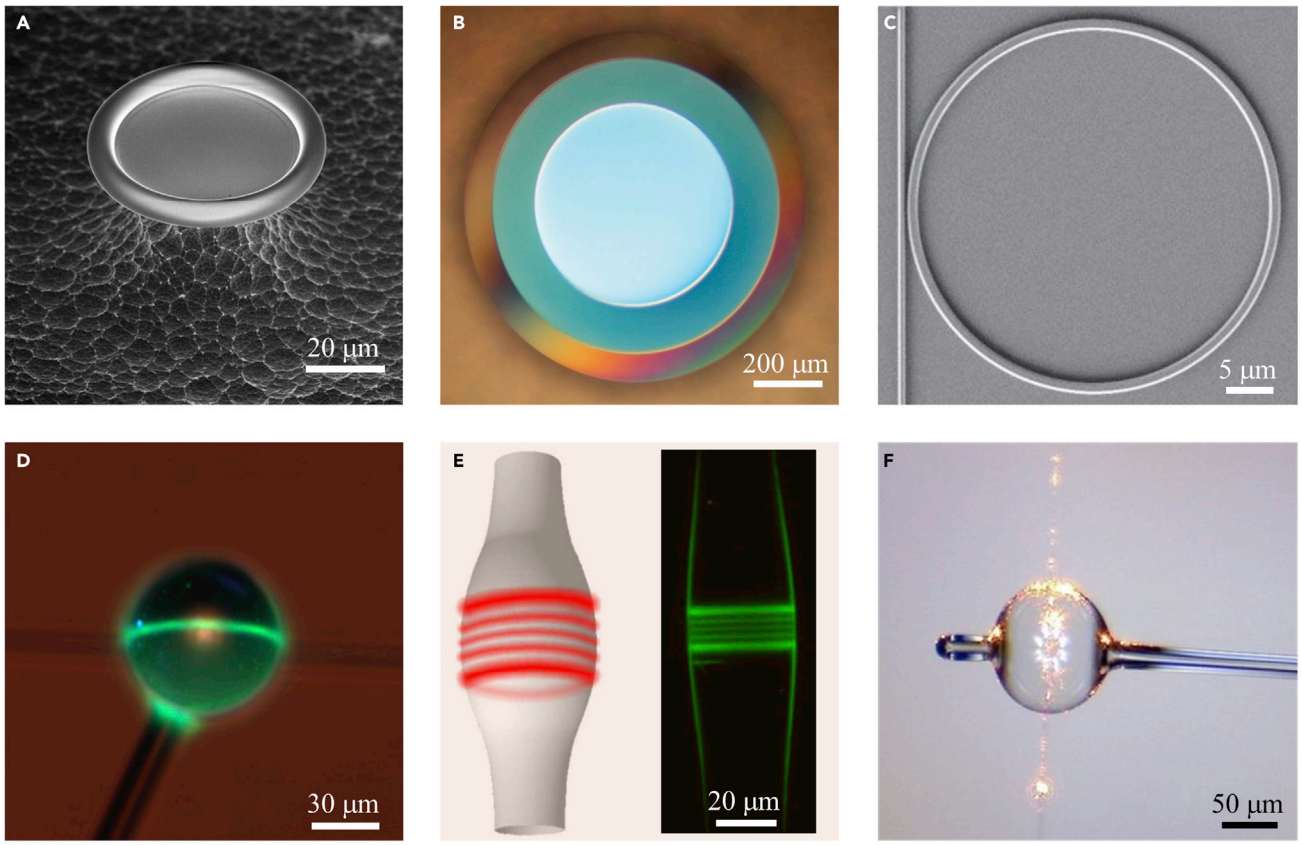

Figure 1. Images of Various Resonator Geometries
(A) Microtoroid,[6] (B) microdisk,[7] (C) microring,[8] (D) microsphere,[9] (E) microbottle,[10] and (F) microbubble.[11]

high-finesse microcavities allow light to interact with the analytes or targets of interests millions of times, dramatically improving the sensitivity of the sensors. The ultra-high quality factor (*Q*), the relatively small mode volume, and various morphologies and versatile materials available to form WGM resonators have led to rapid advances in the field of WGM resonator-based optical sensing.

Various WGM microresonator structures have been employed for sensing, including chip-based and free-standing WGM microresonators, as shown in Figure 1. Common structures for chip-based WGM microresonators are microdisks, microrings, and microtoroids. Free-standing WGM resonators include microspheres, microbottles, and microbubbles. Among them, microtoroids, microspheres, microbottles, and microbubbles possess the highest-quality factors,[4] up to 10^{10}, due to a special laser reflow process that results in a cavity structure with atom-scale surface roughness.[5] It is worth noting that microbubble resonators are hollow and can be filled with either liquid or gas, which gives them a clear advantage in analyte delivery, especially when they are integrated with microfluidic systems.

WGM devices were initially used to study microlaser and nonlinear optics.[12–16] Interest in sensing began in 2002 when the detection of a protein monolayer using a microsphere resonator was demonstrated.[17] Since then, there have been many significant progresses in resonator designs and signal enhancement techniques, enabling the detection of single nanoparticles, viruses, proteins, nucleic acids, and even individual ions, as shown in Figure 2. WGM resonators can detect not

[1]Department of Electrical and Systems Engineering, Washington University in St. Louis, St. Louis, MO 63130, USA

[2]School of Applied and Engineering Physics, Cornell University, Ithaca, NY 14853, USA

*Correspondence: yang@seas.wustl.edu

https://doi.org/10.1016/j.matt.2020.07.008

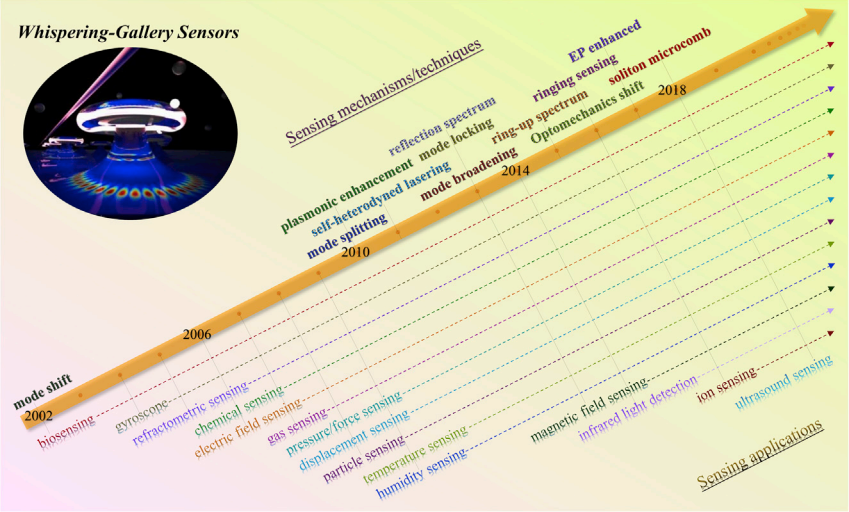

Figure 2. Sensing Mechanisms and Techniques for Whispering-Gallery Mode Sensors, and the Development of Different Sensing Applications in the Last Two Decades

only physical matter but also invisible stimuli such as electrical and magnetic fields, pressure and force, and temperature changes by taking advantage of various morphologies and materials specifically designed to be responsive to each of these stimuli.

In this review, we provide an overview of the sensing mechanisms for WGM resonator sensors as well as the various enhancement techniques used for myriad applications. We also offer our critical evaluation of the challenges and prospects of this exciting research area.

SENSING MECHANISMS AND ENHANCEMENT TECHNIQUES

Mode Shift

In mode shift sensing, changes in the resonant wavelength of WGMs are used to measure the signal of interest.[18] These sensing tests are often implemented by monitoring changes of resonances in the resonator's transmission, reflection, or emission spectra, but can also be measured by fixing the probe wavelength within a resonance and observing changes induced by resonance shifts in the transmission. Mode shift is the most commonly used sensing modality for WGM resonators, due to its applicability to a broad range of analytes. It can be used to measure both the adsorption of analytes[18] and refractive index changes surrounding the microresonator.[19] Mode shift sensing is also used to detect changes in physical parameters surrounding the WGM device, such as heat,[20] pressure, force,[21] and magnetic fields.[22] For example, Figure 3G shows a thermal shift sensing experiment by a silk microtoroid.[23] The mode shift observed in WGM resonators due to the adsorption of an analyte can be understood by the reactive sensing principle.[1] Intuitively, when a particle with a refractive index greater than the medium around the resonator is adsorbed on the resonator, it pulls a part of the resonator's optical field outward, increasing the optical path length and leading to a red shift in the resonance mode.

The acquisition time of mode shift sensing, which requires frequency scanning of the probe laser, is usually on the order of tens of milliseconds and is limited by the frequency modulation bandwidth of the laser. An alternative method to improve time resolution is the mode-locking technique. Specifically, the probe laser frequency

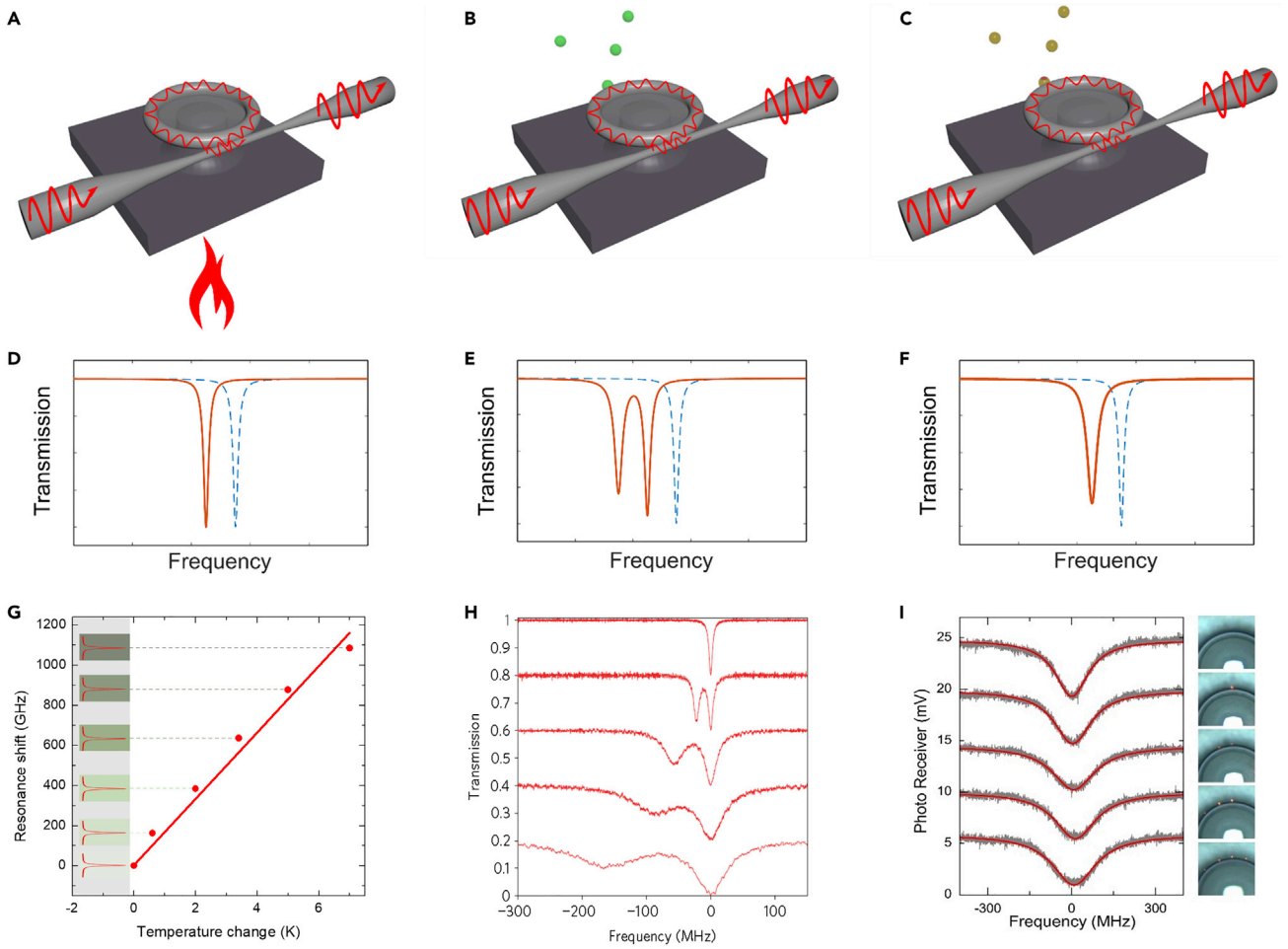

Figure 3. Fundamental WGM Sensing Mechanisms

Fundamental sensing mechanisms (A–F) and corresponding applications (G–I) of the WGM sensor, including mode shift (A and D), mode splitting (B and E), and mode broadening (C and F). (G) Thermal shift sensing using a silk microtoroid resonator.[23] (H) Mode splitting induced by individual polystyrene (PS) nanoparticles.[24] (I) Mode broadening spectra induced by single nanoparticles.[25]

is locked to the resonant frequency of a WGM by the Pound-Drever-Hall technique.[26,27] The amplitude of a feedback error signal proportional to the frequency difference of the probe laser and resonant mode is monitored to extract the resonant mode shift signal, allowing for a time resolution as short as 1.2 ms.[26]

The mode shift sensing mechanism can be applied to not only the optical modes but also optomechanical modes, demonstrated in both microsphere[28] and microcapillary[29–31] resonators. Specifically, an optomechanical spring effect is used in the optomechanical mode shift, in which single-particle or single-molecule-induced optical resonance shift was converted to the mechanical resonant frequency shift. Optomechanical sensing can produce faster sensing via the ultrafast speed of the real-time electronic spectrum analyzers.

Mode Splitting

In a WGM resonator without scatterers, resonant modes exist in pairs of degenerate modes: the clockwise (CW) propagating modes and counterclockwise (CCW) propagating modes. When a nanoscatterer is introduced onto a resonator, part of the

light scattered from the CW mode can be scattered into the CCW mode, and vice versa, inducing coupling between the two modes. Due to this coupling the degeneracy between the two modes is lifted, leading to a split in the resonance mode, as shown in Figures 3E and 3H. By measuring the resonant mode splitting, the presence of the scatterer can be detected.[24] The mode-splitting mechanism has been demonstrated to detect nanoparticles on the order of tens to hundreds of nanometers with a visible or near-infrared probe laser.[24,32–34] One of the advantages of the mode-splitting mechanism is its ability to perform self-referenced detection, which is not influenced by thermal or pressure fluctuations. It is also possible to determine the size of particles adsorbed to the resonator surface derived from the mode-splitting spectra.[35]

Recently, a mode-splitting mechanism in an optomechanical mode has been used to retrieve the eigenfrequencies of bacteria's low-frequency vibration modes.[36] Low-frequency vibration modes of bacteria carry information on their structure and mechanical properties relevant to the biological states. In this work,[36] Gil-Santos et al. deposit a bacterium on the surface of an ultrahigh frequency optomechanical microdisk resonator. When the frequencies of vibration modes of the disk and bacterium are similar, two mechanical modes couple and then split into two collective eigenmodes. By analyzing the mechanical mode splitting and the linewidth broadening, the eigenfrequencies and mechanical loss of the bacterium low-frequency vibration modes could be retrieved.

Mode Broadening

The mode linewidth broadening sensing mechanism is used to measure either scattering loss or absorption loss caused by analytes such as single nanoparticles and single biomolecules, and refractive index changes. Similar to mode splitting, this technique is a self-referenced detection mechanism, isolating the fluctuation of environment temperature or system instability. Furthermore, it removes the requirement of narrow linewidth (ultrahigh Q) needed to resolve the doublet in the splitting spectrum. Experimentally, Shao et al. reported the detection and counting of single 70-nm-radius polystyrene (PS) nanoparticles and lentiviruses by monitoring the linewidth broadening in a free-space coupled deformed microresonator,[25] as shown in Figure 3I. Also, Armani and Vahala demonstrated the detection of heavy water with a volume concentration of 0.0001% D_2O (v/v) in H_2O by monitoring the absorption induced linewidth narrowing (i.e., Q factor increase).[37] Shen et al. demonstrated the detection of single lossy nanoparticles using the dissipative interaction in a high-Q toroidal microcavity.[38]

Ring-Up Spectroscopy

Although submillisecond time resolution can be achieved with mode-locking techniques, it can only be used to measure the resonant frequency shift of a WGM. Cavity ring-up spectroscopy, on the other hand, provides a solution to measure the mode shift and splitting/broadening signals simultaneously.[39] This technique offers a time resolution as short as 16 ns per frame. Specifically, blue-detuned probe laser pulses are coupled with the modes, resulting in the build-up of a transient field in the cavity, which interferes with the transmitted field to create a ring-up signal, as shown in the center inset of Figure 4. In the ring-up signal, the detuning, δ, from the probe is exhibited by the fast oscillations; the resonance width, 2κ, is derived from the exponential decay envelope; the slow beat note indicates the splitting of the resonance, $2g$. This technique has been used to measure fast optomechanical oscillations in the range of megahertz at a time resolution of 16 ns. Cavity ring-up spectroscopy provides an opportunity for optical WGM sensing with nanosecond time resolution

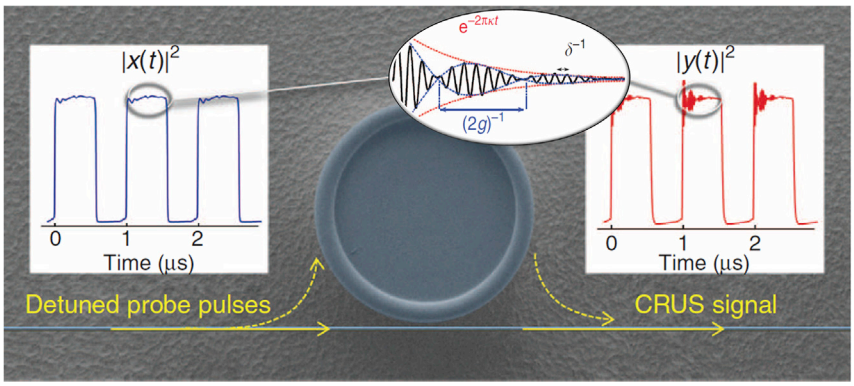

Figure 4. Schematic of Ring-Up Spectroscopy Sensing Mechanism

Sharply rising detuned probe pulses (left inset) lead to the build-up of a cavity field. As this weak field leaks back into the fiber, it interferes with the probe, resulting in a beating signal at the output (right inset). The resonance width, 2κ, the detuning, δ, and the splitting of the resonance, $2g$, can be derived from the ring-up signal.

and holds great potential to detect single-nanoparticle or single-molecule movement by deriving the signals of the mode shift and splitting/broadening from the ring-up signal.

Plasmonic Enhancement

When light is incident on gold or silver nanoparticles, the free electrons in the metallic nanoparticles oscillate with the incident optical field, forming localized surface plasmon (LSP) resonance. LSP resonance is manifested as an intense electromagnetic field, i.e., plasmonic hotspots,[40,41] around the nanoparticles. When a molecule of interest enters the plasmonic hotspots, it interacts strongly with the enhanced electromagnetic field, leading to a visible change in the plasmonic signals. By integrating the LSP resonance with a WGM resonance, a highly sensitive sensing platform has been demonstrated to detect single molecules (Figure 5A).

Early work on hybrid plasmonic WGM resonators for sensing demonstrated the detection of single PS nanoparticles, single virus particles (Figure 5B), and proteins in solution with enhanced sensitivity.[40,41] The first single-protein detection using a hybrid plasmonic WGM resonator was demonstrated by Dantham et al. using gold nanoshells.[40] These authors noted that the large enhancement in sensitivity was attributed to hotspots contributed by bumps on the nanoshell. Later, Baaske et al. demonstrated the measurement of single nucleic acids[42] and even single atomic ions[43] using a hybrid gold nanorod-WGM resonator, marking the highest sensitivity achieved by WGM resonators so far (Figures 5C and 5D). In these works, the detection of single molecules appeared as either spike or step changes, corresponding to transient or semi-permanent binding events. The statistics of this type of binding events provide information of the binding affinities of molecules[44] and lay the foundation to study molecular interactions on surfaces.

Gain and Lasing Enhancement

The detection limit of a WGM sensor depends on the linewidth of the mode, as the linewidth is related to the resolvability of split modes or resonance shifts. This detection limit can be improved significantly by using optical gain to decrease the resonance linewidth by compensating the losses. For example, the laser linewidth is much narrower than the corresponding passive cavity linewidth.[45] Experimentally,

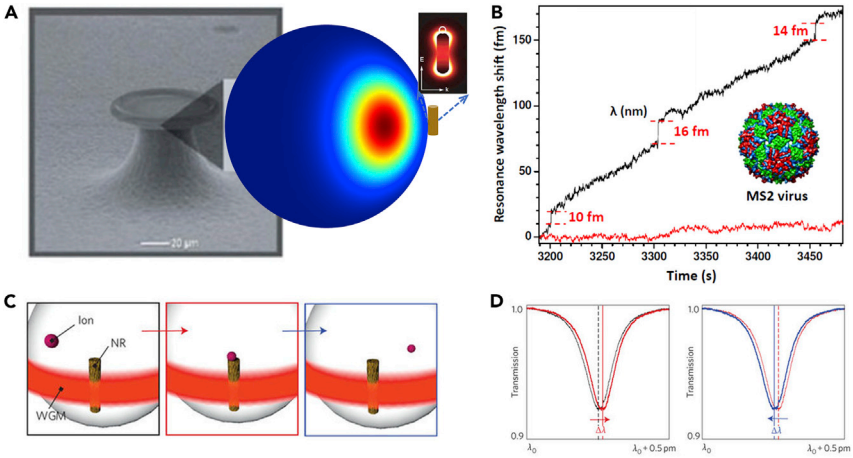

Figure 5. Plasmonic Enhanced WGM Sensing

(A) Scanning electron microscopy (SEM) image of a microtoroid coupled with an Au nanorod (NR). Insets: electric field intensity distributions of an NR and WGM.

(B) Resonance wavelength shift when individual MS2 viruses bind to a microsphere with a gold nanoshell attached on its equator. The control experiment, without the nanoshell or the MS2 virus is shown by the red curve.

(C and D) Plasmonic enhanced transient sensing. Transient interactions of single ions with the NRs (C), excited at their plasmon resonance, are detected as a red shift of the WGM resonance (D, left) when an ion enters a sensing site on an NR's surface, and a subsequent blue shift (D, right) when the ion leaves the sensing site.

the gain in the silica microcavity can be provided by either rare-earth ion doping, such as erbium, yttrium, or thulium, or via stimulated Raman scattering operating at any wavelength. The direct measurement of mode-splitting spectrum through the lasing spectra is typically not possible, since the laser splitting is smaller than the resolution of optical spectrometers. Instead, the mode splitting is measured through observing the beating in the laser output. When a nanoparticle or molecule moves into the mode volume of the WGM, the laser spectrum splits. The split laser modes lead to a self-heterodyned beat note with a frequency that is equal to the difference in frequency between the two laser modes. Furthermore, the lasing spectrum and the frequency of the beat note change again when a second nanoparticle binds. Accordingly, individual nanoparticles can be continuously detected in real time by monitoring the beat note signal,[32] as shown in Figure 6A. Furthermore, self-heterodyned mode splitting in a WGM Raman microlaser for the detection of single nanoparticles down to 10 nm has also been realized experimentally by several groups.[46,47]

Exceptional Points Enhancement

Optical cavities operating at non-Hermitian spectral degeneracies known as exceptional points (EPs) have demonstrated non-trivial physical features, such as chiral modes and anomalous behaviors in lasers.[49,50] It has been recently demonstrated that at such EPs, the scatterer-induced mode splitting can be enhanced.[48] The enhancement comes from the square-root dependence of mode splitting on particle-induced perturbation near second-order EPs as opposed to the linear dependence in conventional cavity sensors, as shown in Figure 6B. This enhancement in sensitivity is greater for smaller perturbations, which has been experimentally demonstrated by tuning WGM to an EP with two nanotips. Single PS nanoparticles with EP-enhanced sensitivity have also been detected in a microtoroid resonator (Figure 6B).

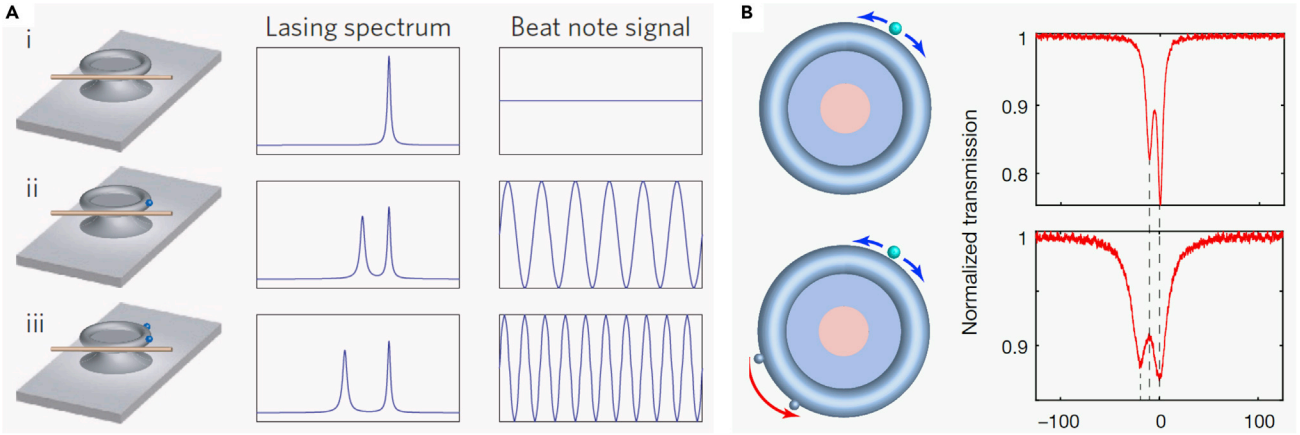

Figure 6. Mode-Splitting Sensing Enhancement Mechanisms

(A) Self-heterodyned microlaser detection of a single nanoparticle.[32] (i) Before nanoparticles arrive, a single mode appears in the lasing spectrum and the laser intensity is constant. (ii) The lasing mode splits into two modes when the first nanoparticle binds, leading to a beat note at a frequency that is equal to the frequency difference between the two modes. (iii) The lasing spectrum and the frequency of the beat note change again when a second nanoparticle binds.

(B) Sensitivity enhancement at exceptional points.[48]

SENSING PARAMETERS

Sensitivity

The sensitivity of an optical sensor is usually defined as the ratio of signal changes from the sensor to the variation in the measured parameter. Taking a WGM thermal sensor for instance; if the resonant wavelength of a particular WGM shifts 1 nm when the temperature changes by 1 K, the sensitivity will be 1 nm/K. Note that the sensitivity is mainly determined by the properties of the sensor, while the detection limit depends on both sensitivity and noise levels. The sensitivity of a WGM thermal sensor relies on the material properties of the cavity, including both the thermo-optic coefficient and the thermal expansion coefficient. In principle, cavity material with a larger thermo-optic coefficient and thermal expansion coefficient will lead to a larger resonant wavelength shift and thus possesses a higher sensitivity.

Taking single-molecule or single-nanoparticle sensing as another example, the single-nanoparticle or single-molecule-induced mode shift, splitting, or broadening signals depend mainly on the relative electric field strength at the position of the molecule as well as the mode volume. Therefore, any techniques with the capability of increasing the relative electric field or decreasing the mode volume will significantly boost the sensor's response to individual analytes. For example, metal nanostructures with surface plasmon resonances provide a huge enhancement of the electric field near the nanostructures and could significantly enhance the sensitivity of all three sensing mechanisms. In addition, for mode-splitting sensing mechanism, the complex square-root topology near EPs also has great potential for enhanced sensitivity.[48,51] Numerical simulations have demonstrated a 7-fold enhancement of the sensitivity for mode splitting.[52] It is worth noting that usually a higher *Q* factor or related gain and lasing enhancement will help lower the detection limit but will not lead to a higher sensitivity. However, in a mode shift sensing mechanism, if we define the sensing signal as the transmitted light intensity at a fixed frequency within the resonance instead of the resonant frequency, a higher *Q* factor mode or a Fano resonance[53,54] will possess a higher sensitivity.

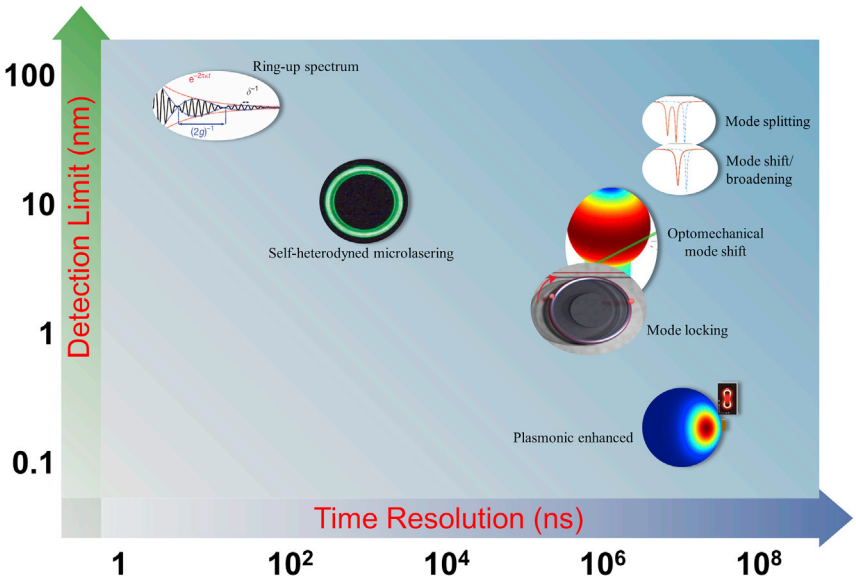

Figure 7. Time Resolution and Detection Limits of Selected Sensing Mechanisms and Enhancement Techniques

Time Resolution

The time resolutions of most WGM sensing mechanisms are on the order of tens of milliseconds, which are limited by the frequency modulation bandwidth of the laser instead of the WGM sensor itself. To improve the time resolution, one can increase the laser sweep speed or utilize techniques that do not require laser scanning. The frequency modulation bandwidth of a tunable laser is typically on the order of kilohertz, corresponding to a time resolution of submillisecond. On the other hand, to remove the requirement of frequency sweeping, several techniques have been developed, such as mode locking, optomechanics sensing, self-heterodyned microlaser, and cavity ring-up spectrum. The time resolution of the mode-locking sensing technique is about 1 ms, limited by the low-pass filter in the locking system.[26,27] For the optomechanical mode shift sensing, the time resolution is also around several milliseconds but limited by the electrical spectrum analyzer (ESA),[28,29] which can be further improved by a real-time ESA. The self-heterodyned microlaser technique can also achieve near real-time sensing by locking the frequency of the probe laser to a resonant mode. The time resolution is then mainly limited by the data-acquisition system and can be on the order of microseconds.[32] The current state-of-the-art time resolution is as short as 16 ns, which is achieved by the cavity ring-up spectroscopy system.[39] Figure 7 briefly summarizes both the time resolution and the detection limit for single-nanoparticle sensing of several sensing mechanisms and enhanced techniques.

Stability and Detection Limit

One of the features of WGM sensors is their response to any environmental changes that influence the refractive index, which could be used for numerous sensors. On the other hand, this susceptibility to the environment becomes a source of noise in sensing experiments, which needs to be extracted from these background fluctuations. For example, the detection limits of WGM biosensors based on mode shift are typically limited by environmental noises, such as the temperature, mechanical perturbations, and probe laser instability. In contrast, mode splitting[24] and

broadening[25] are immune to these environmental background noises due to their intrinsic self-reference properties.

To minimize the thermal noise in mode shift, including both laser-induced heating and environmental thermal drift, a variety of techniques have been developed.[55] For example, Grudinin et al. compensated probe laser scanning induced heating by applying a second stabilization laser sweeping in the opposite direction.[56] He et al. demonstrated a thermo-optic compensation technique by coating a thin layer of polydimethylsiloxane (PDMS),[57] whose thermo-optic coefficient is contrary to silica, onto the surface of the silica microtoroid. In addition, compensation of thermal effect by surrounding medium has also been demonstrated in liquid core microring[58] and microsphere[59] resonators to reduce the sensitivity of WGMs to thermal fluctuations. Furthermore, self-referenced temperature-stabilization techniques down to nanokelvin precision have been developed by monitoring the TE and TM modes simultaneously.[60,61] Multimode sensing for multiparameter measurement has also been demonstrated to improve the stability and detection limit, since the multimode sensing approach can provide abundant and multidimensional sensing information.[62–64]

Specificity

The specificity of WGM microresonators largely depends on the chemical composition and functionalization of the device. A myriad of materials have been utilized to make WGM microresonators to increase the potential chemical functionalizations and capture agents possible. There have been WGM microresonators composed of silica, silicon, CaF_2, PDMS, lithium niobate, and even silk. The native surface of these devices also influences the amount of nonspecific adsorption and fouling that can occur at the surface.

Specificity for WGM microresonators is generally imbued via chemoresponsive elements attached to the surface of the device. For chemical species these include polymer films, brushes, and aptamers. In contrast, for biological molecules, the capture agent of interest is determined by the target molecule. For proteins, antibodies or aptamers are the typical capture agent of interest, while for nucleic acids, complementary strands of nucleic acids (cDNAs or locked nucleic acids) are typically employed, as shown in Figure 8. These capture agents not only affect the specificity of measurements but result in inherent limitations to the binding of target molecules at equilibrium.

Another factor that influences the specificity of WGM microresonators is the medium in which detection is occurring. For sensing in gases or buffered solutions, the risk of "fouling," that is, nonspecific adsorption of molecules to the sensor surface, is minimal. In contrast, measurements in complex medium, such as whole blood, run the risk of significant "fouling" and nonspecific adsorption.

SENSING APPLICATIONS

In this section, we divide the WGM sensing applications into two categories, sensing of physical matters or physical parameters surrounding the resonator that influence the modes. The physical matter can be nanoparticles, small bio/chemical molecules, gas, or any other matter adsorption. On the other hand, the WGM device is also used to detect changes in physical parameters surrounding the WGM device, such as temperature, pressure, force, electric field, magnetic field, or other physical field perturbation. The two WGM sensing categories are summarized in Figures 9 and 10.

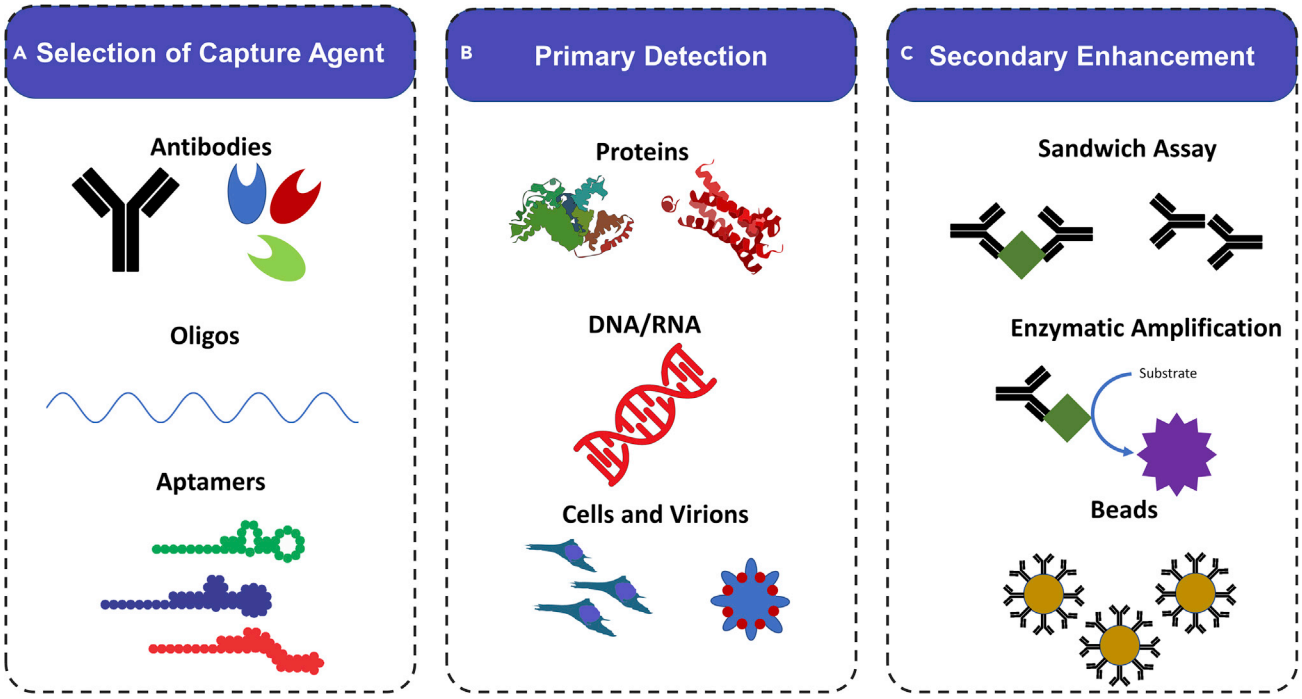

Figure 8. Schematic Detailing the Selection of Capture Agents for Biological Sensing Applications
Depending on the target molecule of interest, a variety of capture agents can be employed (A). Following primary detection (B), additional amplification steps can be pursued to further enhance the sensor response or specificity (C).

Nanoparticle Detection Down to Single Molecules

The sensing of nanoparticles in the size range of tens to hundreds of nanometers represents a model system to study the use of WGM resonators for sensing applications.[74–77] It is important for environmental monitoring and disease control to study atmospheric aerosol particles and virion particles. The detection of single influenza A virion particles (approximately 50 nm in radius) using the mode shift technique was first reported by Vollmer et al. in 2008.[18] Since then, virus particle sensing has been demonstrated with mode-splitting,[32] mode-broadening,[25] and hybrid WGM-plasmonic sensing mechanisms.[78] The mode-splitting technique is particularly well suited for the detection of nanoparticles because the particle-scattering-based mode-splitting signal is unaffected by environmental perturbations (Figure 9C). In addition, real-time sizing of the particle size is possible from the measurement of mode splitting.[24,35]

The sensitivity of WGM sensors has improved greatly in recent years, reaching single-molecule levels. In WGM sensing, single molecules, such as proteins and oligonucleotides, can be thought of as nanoparticles, and their detection is based on the polarizability of each molecule, just like nanoparticles. To enhance the sensitivity of WGM sensors to single-molecule level, an effective strategy is to attach gold nanoparticles to the WGM resonator, using the hybrid resonance between plasmonic resonance in gold nanoparticles and WGM resonance to enhance the wavelength shift. Dantham et al. first reported this strategy for single-molecule detection using gold nanoshells in 2013, demonstrating the detection of single BSA proteins (66 kDa).[40] Baaske et al. further lowered the limit of detection using gold nanorods, demonstrating the observation of individual DNA hybridization events with 8-mer oligonucleotides (2,350 Da).[42] Later, Baaske et al. further showed that, remarkably,

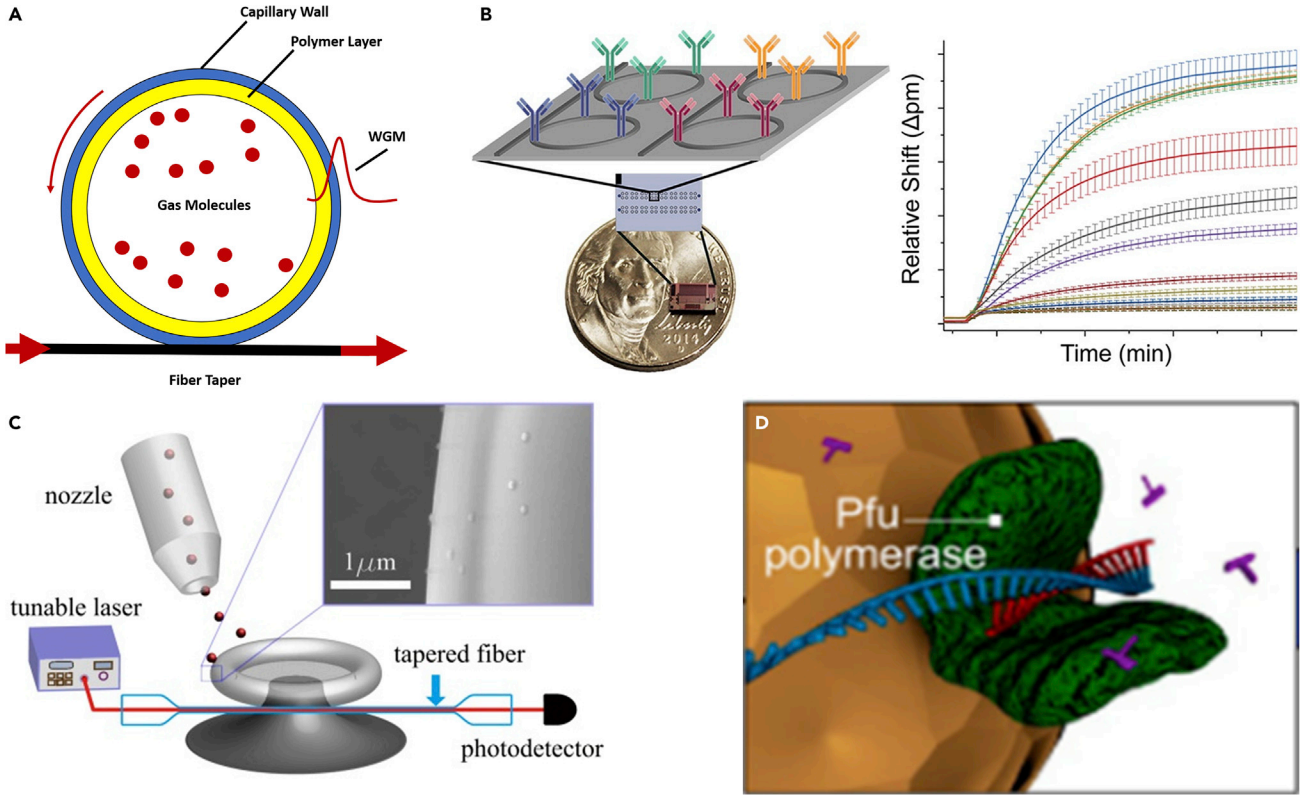

Figure 9. Schematics of WGM-Based Physical Matter Sensing

(A) Detection of gas molecules with an LCORR (liquid core optical ring resonator) configuration, using a chemoresponsive polymer layer.[65]

(B) Biomolecule sensing. (Left) Array of microring resonators, each functionalized with a unique capture antibody, and comparison of the chip size with a nickel for scale. (Right) Kinetic binding curves for the microring array.[66]

(C) Nanoparticle-based sensing system. Inset: SEM image of PS nanoparticles on the surface of toroid.[32]

(D) Medical sensing application. Single enzyme activity of Pfu polymerase attached to a gold nanorod.[67]

even the movement of single atomic ions (Zn and Hg) can be seen as spike and step transitions in the resonance wavelength.[43] Single-molecule detection without using plasmonic nanoparticles has also been reported by Su et al.[27] In this work, the authors used laser-frequency locking to increase the signal-to-noise ratio, demonstrating the detection of human interleukin-2 protein (15.5 kDa) using bare microtoroids. The detection limits of single nanoparticles or molecules for different sensing mechanisms and enhanced techniques are summarized as in Figure 7.

In addition to the direct optical measurement based on particle polarizability, it is also worth noting two indirect particle-detection techniques. One is WGM resonator-based absorption spectrometry, whereby a pump laser is used to heat the nanoparticles and the dissipated heat is sensed by monitoring the WGM resonance shift using a probe laser.[79–82] The signal is based on optical absorption, making this technique especially suited for studying nanoparticles made of absorbing materials such as gold and conjugated polymers. Another indirect technique is based on the optomechanical coupling between optical WGM resonances and long-range phonons, enabling the measurement of particle mass density, mechanical compressibility, and viscoelasticity.[29,83] Both of these techniques measure physical quantities other than particle polarizability and have the potential to expand the versatility of WGM sensors further.

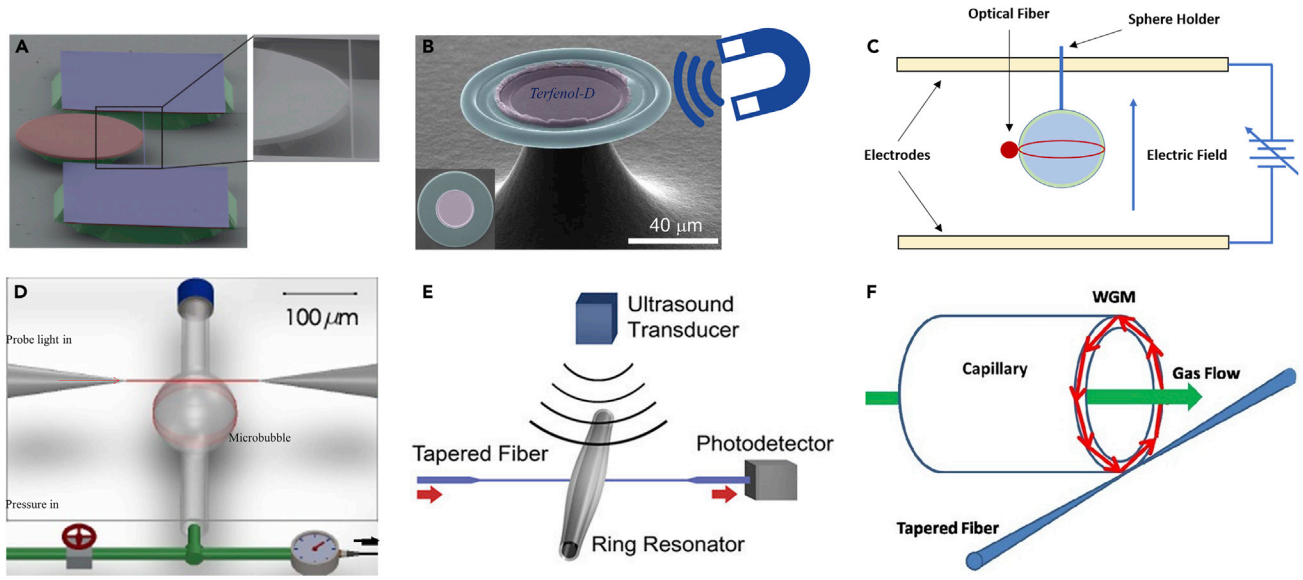

Figure 10. Experimental Set-ups and Images of WGM-Based Physical Parameter Sensing
(A) Force,[68] (B) magnetic fields,[69] (C) electric fields,[70] (D) pressure sensing,[71] (E) acoustic wave sensing,[72] and (F) flow sensing.[73]

In terms of resonator geometry, most of the work on single-particle and single-molecule detection has been based on either microspheres or microtoroids. Recently, detection using hollow microbubble resonators has gained much interest.[81,84] Nanoparticle dispersed in aqueous medium can be conveniently introduced into these hollow resonators, allowing for greater overlap between nanoparticles and WGM evanescent fields, as well as facile handling of fluid samples.

Biological Sensing

One area in which WGM sensors have attracted significant attention is within biological sensing applications. The ability to integrate these devices onto chips, with high sensitivity and low analyte volume requirements, makes them especially appealing for biological applications, in which samples are often limited.

Proteins are the most frequent biomolecule detected with WGM devices. Initial studies demonstrated exquisite sensitivity of WGM devices toward proteins, although these were typically performed in neat buffered solutions, and in many cases without specific capture agents.[85] A number of groups have demonstrated the direct detection of protein in both neat buffered solutions and complex media.[86,87] In these experiments, a capture agent, typically an antibody or aptamer, is attached to the device surface, which provides specificity, as shown in Figure 9B. To further enhance sensitivity as well as specificity in complex media, researchers have also employed a number of secondary enhancement steps, including a combination of sandwich assays, enzymatic reactions,[88] and beads.[87,89]

Another class of biomolecules that has been extensively studied with WGM devices is nucleic acids. Several groups have demonstrated the label-free detection of DNA and RNA with WGM devices.[90–92] Techniques have also been employed to further increase the analytical sensitivity for nucleic acids, either through the additional secondary labels and/or enzymatic reactions.[93,94]

WGM devices have also been used as a method for detecting entire cells and virions. Anderson and colleagues demonstrated the nonspecific binding of *Helicobacter hepaticus*.[95] Ghali et al. used a phage-specific protein to capture *Staphylococcus aureus* onto a microdisk.[96,97] Gohring and Fan were able to detect and subtype human T cells.[98] WGM devices have been applied toward the detection of influenza A, M13, and the Bean pod mottle virus.[18,25,32,35,99,100]

The versatility of WGM devices in biosensing applications is evident not only in that researchers have pushed toward the development of clinically relevant, multiplexed assays, but also in that the devices have also been used to study fundamental mechanisms of biological molecules. For example, Kim and colleagues demonstrated the ability to study the interactions between DNA and a polymerase molecule, utilizing a gold nanorod attached to a microsphere for plasmonic enhancement,[67] as shown in Figure 9D.

Medical Applications

One of the most promising areas for the application of WGM devices lies within medicine. The remarkable sensitivity of the devices, coupled with their relatively low fabrication costs and small volume, makes them an ideal platform for incorporation into clinically relevant technologies and settings.

WGM sensors have demonstrated the ability to detect numerous analytes and signals that would be of significant interest to the medical community. As mentioned previously, researchers have demonstrated the ability of WGM sensors to detect biomarkers, including proteins, nucleic acids, and entire cells or virions. In the context of all biomarkers, it is important to compare the performance of WGM sensors relative to field standards. In the context of protein detection, ELISAs are typically employed in clinical settings, often utilizing an amplification step. Where WGM sensors excel, in general, is the ability to offer improved-sensitivity (both label-free and with amplification techniques) multiplexed measurements toward different targets simultaneously, as well as faster time to results.[88,101] For both nucleic acids and viruses, the gold standard within many medical applications is PCR-based techniques. WGM devices have difficulties in competing with the ultimate sensitivity of PCR techniques (a single copy). However, in the direct, unamplified detection of nucleic acids or virion particles, WGM devices have demonstrated superior performance. In particular, the ability to directly detect virions for influenza A, M13, and the Bean pod mottle virus highlights a potential niche in which WGM sensors might be employed in point-of-care applications for the rapid detection of viruses.[18,25,32,35,78,99]

While not quite yet fully realized, another area in which WGM sensors are entering the medical domain is through the uses of protein nanodisks, scaffolds of proteins supporting cell membranes.[102] The ability to couple nanodisks to WGM sensors enables the study of cell membrane proteins, critical in a variety of therapeutics. Muehl et. al. demonstrated an application of this technique to assess the binding between prothrombin, factor X, activated factor VII, and activated protein C to varying lipid concentrations in nanodisks.[103] The ability to create protein nanodisks may also enable researchers to study a wide range of transmembrane proteins and ion channels. As many significant drug targets rely on transmembrane proteins or ion channels for their action, this enables the study of drug interactions at a level previously unavailable.

Outside of biomarkers, WGM sensors have also been applied toward the detection of signals used with medical devices. For example, Basiri-Esfahani and colleagues

demonstrated the ability to leverage microdisk devices for the detection of ultrasound.[104] Their sensors reported a force sensitivity of 370 fN/Hz$^{1/2}$, an improvement of more than three orders of magnitude over high-sensitivity piezoelectric sensors, which are currently used in ultrasound devices. The ability to detect magnetic fields also has enormous potential in the context of magnetic resonance imaging (MRI) techniques. While WGM sensors are still naive in the context of these technologies, their enormous improvements in sensitivity and performance metrics have the potential to transform the use of these techniques. Of particular interest is the small size of WGM sensors coupled with the potential to be multiplexed. Together, these qualities of WGM sensors enable the technology to be integrated into new medical applications. For example, the ability to build highly multiplexed arrays of magnetometers could enable higher-resolution MRI instruments, in addition to new imaging modalities that are not currently possible with conventional techniques.

With a broad range of analytes WGM sensors can detect, coupled with the ability to miniaturize entire WGM systems into portable devices,[105] there is an enormous potential for these sensors to effect clinically actionable changes within medicine, and this will be an exciting frontier to monitor.

Gas Sensing

Another area of sensing in which WGM devices have been applied is for the detection of gases. The most common experimental set-up is to coat a WGM device with a chemoresponsive layer specific for the gas of interest. Interactions of the target gas with the polymer layer leads to a change in the refractive index of the layer, which is subsequently detected by the WGM device, as shown in Figure 9A. The added benefit is that these polymer layers can provide a level of specificity toward target gases. This has been used by many groups for the detection of a wide variety of analytes,[65,106–108] including ammonia, water, organic compounds, alcohols, and helium/argon. Gas chromatography has also been coupled with WGM devices, whereby a capillary is used as both the medium for the WGM device and separation process.[26] Another approach for the detection of gases involves the use of graphene to generate Brillouin optomechanical modes, which provides even higher analytical sensitivity.[109]

Temperature Sensing

While a significant limitation of many WGM devices is thermal drift, many groups have been able to utilize WGM devices as highly sensitive temperature sensors. Temperature sensing has been demonstrated using silica-based[110,111] and silicon-based[112] devices. However, the thermo-optic coefficient and thermal expansion coefficient of these materials are positive, making it incredibly difficult to separate the two effects of heating with bare silica or silicon alone. Many WGM devices utilized for temperature sensing are composed of materials that offer a larger negative thermo-optic coefficient, including PDMS,[113,114] UV-curable adhesives,[115] lithium niobate,[116] and dye-doped photoresists,[117] which give rise to much higher sensitivity. In addition, materials with a large thermal expansion coefficient, such as silk, have also been used to fabricate a WGM microresonator thermal sensor.[23,118]

Magnetic Field Sensing

Due to the $1/r^3$ decay of dipolar magnetic fields, magnetometer size is one of the critical parameters for improving the sensitivity of sub-femto-tesla magnetometers. Thus, a number of technologies have been developed to achieve higher sensitivity together with smaller sensor sizes. Among them, the WGM microcavity-based optomechanical magnetometer is an encouraging candidate.[22,119,120] Currently, several

types of hybrid magnetometers based on WGM have been developed, such as magnetostrictive material (Terfenol-D) embedded[22] or sputter coated[69] onto the pillar of toroidal microresonators and micromagnets integrated into soft polymer material surrounding a microtoroid.[120] For the Terfenol-D-microtoroid hybrid magnetometer, as shown in Figure 10B, a 585-nT/$Hz^{1/2}$ peak sensitivity has been achieved by Li et al.[69] On the other hand, the micro-magnets-polymer-microtoroid hybrid magnetometer possessing a sensitivity of 880 pT/$Hz^{1/2}$ at a frequency of 200 Hz has also been demonstrated by Zhu et al.[120]

Pressure and Force Sensing

For the detection of pressure and force, there are several configurations utilized by researchers. One configuration involves the use of WGM structures to serve as transducers. Force on the WGM structure itself leads to a change in the device's shape, and mechanical stresses are realized as changes in the refractive index of the device. This technique has been demonstrated with both solid[21,121] and hollow[71,122] resonators, the advantage of the latter being that the hollow structure assists in transducing the pressure for measurement, as shown in Figure 10D. Another technique is to immerse the WGM device into a transduction medium (such as an elastic polymer) or attach the device directly to a polymer transducer.[121] Furthermore, the evanescent field of a WGM resonator comes with a steep gradient, which can be used to detect weak incoherent forces,[68] as shown in Figure 10A. A direct application of pressure-based sensing with WGM devices is acoustic imaging modalities, such as ultrasound,[72] as shown in Figure 10E. Unlike traditional piezoelectric-based sensors currently used, WGM sensors offer the advantage of improved sensitivity as well as operating bandwidth.

Other Sensing Applications

There is an ever-expanding role for WGM microresonators as sensors. While our review has covered some of the more prevalent areas of sensor development, WGM devices have also been applied as sensors for other applications. WGM resonators can be used as a refractive index sensor, which is used to sense the changes in the concentration of analyte in a solution.[123] They have also been used to characterize chemical reactions *in situ*, such as polymerization, gelation, and phase transition in hydrogels.[124,125] By introducing materials that are responsive to physical stimuli such as different polymers, WGM resonators can be made further responsive to electric fields[70,126,127] (Figure 10C) and humidity.[128,129] The circular pass of light in WGM resonators make these resonators analogous to a Sagnac interferometer, and this principle has been used to develop WGM-resonator-based gyroscopes.[130,131] In addition, capillary microring resonators have also been used for the detection of acoustic waves[72] and gas flow rate,[73] as shown in Figures 10E and 10F, respectively. There has been increasing recent interest in soliton frequency combs using high-*Q* microresonators, originating from cascaded four-wave mixing in a WGM microresonator, which has been implemented for ultrafast distance measurements with submicron resolution.[132,133] Furthermore, cavity soliton microcombs have also been used in astronomy in the search for exoplanets.[134] The thermal vibrations of a carbon nanotube have also been monitored in real time by measuring the transmission of a high-*Q* silicon nitride microcavity.[135] We anticipate that the exquisite sensitivity of WGM microresonators will catalyze significant development in these areas moving forward.

CONCLUSIONS AND PERSPECTIVES

Here, we have briefly reviewed the mechanisms, methods, structures, techniques, parameters, and applications of sensors based on WGM microresonators over the last

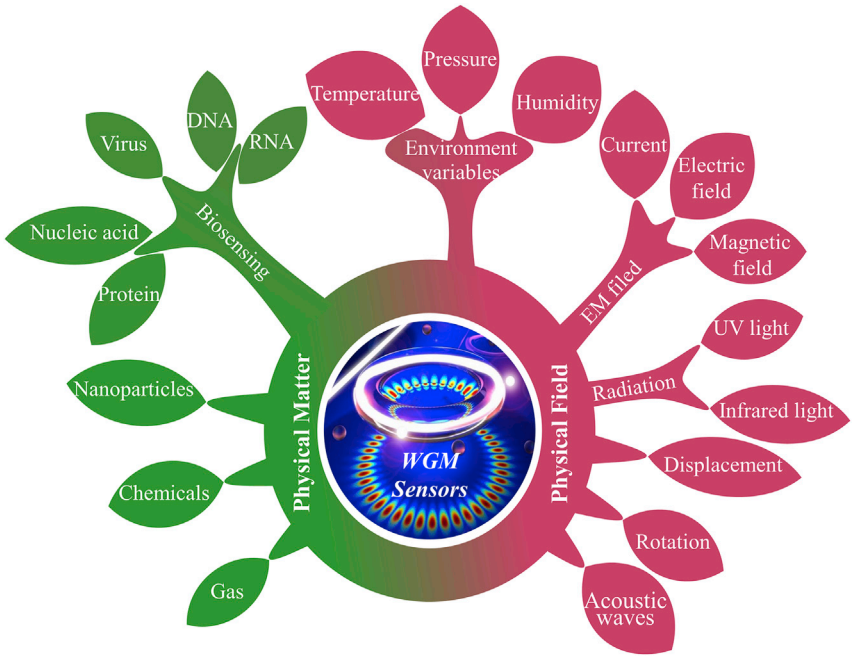

Figure 11. Overview of Sensing Applications of WGM Microresonator

two decades. Arising from the ultrahigh power build-up factors and enhanced light-matter interactions in WGM microresonators, an enormous number of sensing experiments have been demonstrated, including not only traditional physical matter sensing, such as particle, gas, and bio/chemical sensing, but also physical field sensing, for example, temperature, electric field, magnetic field, and pressure, force sensing (Figure 11). Three fundamental sensing mechanisms and several enhanced sensing techniques or mechanisms have been developed in the last two decades, which have been discussed and summarized. In addition, different kinds of WGM structures as platforms for sensing are presented. Some sensing parameters, such as sensitivity, time resolution, stability, and specificity, have been discussed for some sensing techniques or mechanisms.

Looking ahead, there are still many challenges and potential directions for WGM microresonator sensors. Here, we list some potential directions of WGM sensors based on material, structure, mechanism, technique, and integration/encapsulation.

The development of new materials for the targeted detection of specific analytes is always one of the core research fields. For example, materials with electro-optic effects can be used for a microresonator as a high-sensitivity electric field sensor; multilayers of polymers could be coated onto a high-Q microresonator to sense multicomponent gas.

There is still significant progress to be made in the development of WGM microresonator structures, such as deformed microresonators,[136–144] endoscopic sensing probes,[145,146] and WGM sensors in chip-based microfluidics channels.[147] Not only will these lead to further improvement in device sensitivity but they will also allow for the detection of analytes that are beyond the reach of current techniques.

From the sensing mechanism or technique point of view, we envision the development of techniques that allow for the undirected and *de novo* identification and detection of

analytes. This would extend the application of WGM microresonators as a sensor into a new, highly sensitive discovery tool. On the other hand, the development of even more enhancement techniques for sensing purposes is highly desired. As our understanding of the fundamental physics and phenomena of these devices improves, new and innovative methods to improve their optical performance will follow. Furthermore, how to suppress all kinds of noises to achieve a specific sensor is always one of the research hotspots. For example, Hu's group demonstrated a new sensing method by using the waveguide coupled with a cavity as a sensor device instead of the microcavity itself.[148–150] The structure is a microring resonator that is coupled by a sensing arm waveguide two times. When the nanotarget is exposed to the sensing arm waveguide, a tiny variation of the sensing arm waveguide triggers a phase change; this in turn induces a significant change of external effective coupling strength between the waveguide and the microring and, thus, the resonant transmission depths vary, which serves as a sensing signal. The advantage of this dissipative sensing method is its immunity to frequency noises at a high signal-to-noise ratio.

The recent SARS-CoV-2 outbreak highlights a critical need for point-of-care diagnostic tests that can compete with PCR-based methods without the need for amplification or centralized laboratories. This highlights a potential opportunity for WGM sensors, which have demonstrated exceptional sensitivities as well as the ability to be portable.

There is an increased need for the integration and miniaturization of the entire WGM sensing systems,[105] and construction of a sensor network consisting of all kinds of WGM sensors for both environmental and health monitoring. For example, real-time monitoring of the heartbeat and blood pressure by integrating WGM pressure sensors into a wristband or a watch will greatly improve our health status and impact healthcare systems.

The Internet of Things (IoT) monitoring of environmental signals, such as temperature, humidity, and pressure, has promising applications in modern society. Wireless photonic sensors used in the IoT provide a significant advantage in harsh environments due to their immunity to the electromagnetic interference. Among them, WGM photonic sensors, benefiting from their ability of enhancing light-matter interactions, as well as their small size, scalable production methods, and ability to be integrated with conventional electronics, may have particular potential for the next-generation IoT technology.[151]

ACKNOWLEDGMENTS

The authors acknowledge the support from ARO grant no. W911NF1710189 and NSF grant nos. EFMA1641109 and ECCS1711451.

AUTHOR CONTRIBUTIONS

All authors contributed to the preparation of the manuscript.

REFERENCES

1. Vollmer, F., and Arnold, S. (2008). Whispering-gallery-mode biosensing: label-free detection down to single molecules. Nat. Methods *5*, 591–596.

2. Foreman, M.R., Swaim, J.D., and Vollmer, F. (2015). Whispering gallery mode sensors. Adv. Opt. Photonics *7*, 168.

3. Jiang, X., Qavi, A.J., Huang, S.H., and Yang, L. (2018). Whispering gallery microsensors: a review. arXiv, 1805.00062.

4. Gorodetsky, M., Savchenkov, A., and Ilchenko, V. (1996). Ultimate Q of optical microsphere resonators. Opt. Lett. *21*, 453–455.

5. Armani, D.K., Kippenberg, T.J., Spillane, S.M., and Vahala, K.J. (2003). Ultra-high-Q toroid microcavity on a chip. Nature *421*, 925–928.

6. Jiang, X.-F., Xiao, Y.-F., Yang, Q.-F., Shao, L., Clements, W.R., and Gong, Q. (2013). Free-space coupled, ultralow-threshold Raman

lasing from a silica microcavity. Appl. Phys. Lett. *103*, 101102.

7. Lee, H., Chen, T., Li, J., Yang, K.Y., Jeon, S., Painter, O., and Vahala, K.J. (2012). Chemically etched ultrahigh-Q wedge-resonator on a silicon chip. Nat. Photonics *6*, 369–373.

8. Xu, Q., Schmidt, B., Pradhan, S., and Lipson, M. (2005). Micrometre-scale silicon electro-optic modulator. Nature *435*, 325–327.

9. Spillane, S.M., Kippenberg, T.J., and Vahala, K.J. (2002). Ultralow-threshold Raman laser using a spherical dielectric microcavity. Nature *415*, 621–623.

10. Pöllinger, M., O'Shea, D., Warken, F., and Rauschenbeutel, A. (2009). Ultrahigh-Q tunable whispering-gallery-mode microresonator. Phys. Rev. Lett. *103*, 053901.

11. Henze, R., Seifert, T., Ward, J., and Benson, O. (2011). Tuning whispering gallery modes using internal aerostatic pressure. Opt. Lett. *36*, 4536–4538.

12. Ilchenko, V.S., and Matsko, A.B. (2006). Optical resonators with whispering-gallery modes - Part II: Applications. IEEE J. Sel. Top. Quan. Electron. *12*, 15–32.

13. Li, Y., Jiang, X., Zhao, G., and Yang, L. (2018). Whispering gallery mode microresonator for nonlinear optics. arXiv, 1809.04878.

14. Huang, S.H., Jiang, X., Peng, B., Janisch, C., Cocking, A., Kaya Özdemir, S., Liu, Z., and Yang, L. (2018). Surface-enhanced Raman scattering on dielectric microspheres with whispering gallery mode resonance. Photon. Res. *6*, 346–356.

15. Yang, Y., Jiang, X., Kasumie, S., Zhao, G., Xu, L., Ward, J.M., Yang, L., and Chormaic, S.N. (2016). Four-wave mixing parametric oscillation and frequency comb generation at visible wavelengths in a silica microbubble resonator. Opt. Lett. *41*, 5266.

16. Kasumie, S., Lei, F., Ward, J.M., Jiang, X., Yang, L., and Nic Chormaic, S. (2019). Raman laser switching induced by cascaded light scattering. Laser Photon. Rev. *13*, 1900138.

17. Vollmer, F., Braun, D., Libchaber, A., Khoshsima, M., Teraoka, I., and Arnold, S. (2002). Protein detection by optical shift of a resonant microcavity. Appl. Phys. Lett. *80*, 4057.

18. Vollmer, F., Arnold, S., and Keng, D. (2008). Single virus detection from the reactive shift of a whispering-gallery mode. Proc. Natl. Acad. Sci. U S A *105*, 20701–20704.

19. White, I.M., Oveys, H., and Fan, X. (2006). Liquid-core optical ring-resonator sensors. Opt. Lett. *31*, 1319–1321.

20. Carmon, T., Yang, L., and Vahala, K. (2004). Dynamical thermal behavior and thermal self-stability of microcavities. Opt. Express *12*, 4742–4750.

21. Ioppolo, T., Kozhevnikov, M., Stepaniuk, V., Ötügen, M.V., and Sheverev, V. (2008). Micro-optical force sensor concept based on whispering gallery mode resonators. Appl. Opt. *47*, 3009.

22. Forstner, S., Sheridan, E., Knittel, J., Humphreys, C.L., Brawley, G.A., Rubinsztein-Dunlop, H., and Bowen, W.P. (2014). Ultrasensitive optomechanical magnetometry. Adv. Mater. *26*, 6348–6353.

23. Xu, L., Jiang, X., Zhao, G., Ma, D., Tao, H., Liu, Z., Omenetto, F.G., and Yang, L. (2016). High-Q silk fibroin whispering gallery microresonator. Opt. Express *24*, 20825.

24. Zhu, J., Ozdemir, S.K., Xiao, Y.-F., Li, L., He, L., Chen, D.-R., and Yang, L. (2009). On-chip single nanoparticle detection and sizing by mode splitting in an ultrahigh-Q microresonator. Nat. Photonics *4*, 46–49.

25. Shao, L., Jiang, X.-F., Yu, X.-C., Li, B.-B., Clements, W.R., Vollmer, F., Wang, W., Xiao, Y.-F., and Gong, Q. (2013). Detection of single nanoparticles and lentiviruses using microcavity resonance broadening. Adv. Mater. *25*, 5616–5620.

26. Swaim, J.D., Knittel, J., and Bowen, W.P. (2013). Detection of nanoparticles with a frequency locked whispering gallery mode microresonator. Appl. Phys. Lett. *102*, 183106.

27. Su, J., Goldberg, A.F., and Stoltz, B.M. (2016). Label-free detection of single nanoparticles and biological molecules using microtoroid optical resonators. Light Sci. Appl. *5*, e16001.

28. Yu, W., Jiang, W.C., Lin, Q., and Lu, T. (2016). Cavity optomechanical spring sensing of single molecules. Nat. Commun. *7*, 1–9.

29. Han, K., Kim, J., and Bahl, G. (2016). High-throughput sensing of freely flowing particles with optomechanofluidics. Optica *3*, 585–591.

30. Kim, K.H., Bahl, G., Lee, W., Liu, J., Tomes, M., Fan, X., and Carmon, T. (2013). Cavity optomechanics on a microfluidic resonator with water and viscous liquids. Light Sci. Appl. *2*, e110.

31. Bahl, G., Kim, K.H., Lee, W., Liu, J., Fan, X., and Carmon, T. (2013). Brillouin cavity optomechanics with microfluidic devices. Nat. Commun. *4*, 1994.

32. He, L., Ozdemir, S.K., Zhu, J., Kim, W., and Yang, L. (2011). Detecting single viruses and nanoparticles using whispering gallery microlasers. Nat. Nanotechnol. *6*, 428–432.

33. Kim, W., Özdemir, Ŝ.K., Zhu, J., He, L., and Yang, L. (2010). Demonstration of mode splitting in an optical microcavity in aqueous environment. Appl. Phys. Lett. *97*, 071111.

34. Kim, W., Ozdemir, S.K., Zhu, J., Faraz, M., Coban, C., and Yang, L. (2012). Detection and size measurement of individual hemozoin nanocrystals in aquatic environment using a whispering gallery mode resonator. Opt. Express *20*, 29426–29446.

35. Zhu, J., Özdemir, Ş.K.Ş., He, L., Chen, D.D.-R., and Yang, L. (2011). Single virus and nanoparticle size spectrometry by whispering-gallery-mode microcavities. Opt. Express *19*, 16195–16206.

36. Gil-Santos, E., Ruz, J.J., Malvar, O., Favero, I., Lemaître, A., Kosaka, P.M., García-López, S., Calleja, M., and Tamayo, J. (2020). Optomechanical detection of vibration modes of a single bacterium. Nat. Nanotechnol. *15*, 469.

37. Armani, A.M., and Vahala, K.J. (2006). Heavy water detection using ultra-high-Q microcavities. Opt. Lett. *31*, 1896–1898.

38. Shen, B.Q., Yu, X.C., Zhi, Y., Wang, L., Kim, D., Gong, Q., and Xiao, Y.F. (2016). Detection of single nanoparticles using the dissipative interaction in a high- Q microcavity. Phys. Rev. Appl. *5*, 024011.

39. Rosenblum, S., Lovsky, Y., Arazi, L., Vollmer, F., and Dayan, B. (2015). Cavity ring-up spectroscopy for ultrafast sensing with optical microresonators. Nat. Commun. *6*, 6788.

40. Dantham, V.R., Holler, S., Barbre, C., Keng, D., Kolchenko, V., and Arnold, S. (2013). Label-free detection of single protein using a nanoplasmonic-photonic hybrid microcavity. Nano Lett. *13*, 3347–3351.

41. Swaim, J.D., Knittel, J., and Bowen, W.P. (2011). Detection limits in whispering gallery biosensors with plasmonic enhancement. Appl. Phys. Lett. *99*, 97–100.

42. Baaske, M.D., Foreman, M.R., and Vollmer, F. (2014). Single-molecule nucleic acid interactions monitored on a label-free microcavity biosensor platform. Nat. Nanotechnol. *9*, 933–939.

43. Baaske, M.D., and Vollmer, F. (2016). Optical observation of single atomic ions interacting with plasmonic nanorods in aqueous solution. Nat. Photonics *10*, 733–739.

44. Kim, E., Baaske, M.D., and Vollmer, F. (2016). In situ observation of single-molecule surface reactions from low to high affinities. Adv. Mater. *28*, 9941–9948.

45. He, L., Özdemir, Ş.K., Zhu, J., and Yang, L. (2010). Ultrasensitive detection of mode splitting in active optical microcavities. Phys. Rev. A Mol. Opt. Phys. *82*, 053810.

46. Li, B.-B., Clements, W.R., Yu, X.-C., Shi, K., Gong, Q., and Xiao, Y.-F. (2014). Single nanoparticle detection using split-mode microcavity Raman lasers. Proc. Natl. Acad. Sci. U S A *111*, 14657–14662.

47. Özdemir, Ş.K., Zhu, J., Yang, X., Peng, B., Yilmaz, H., He, L., Monifi, F., Huang, S.H., Long, G.L., and Yang, L. (2014). Highly sensitive detection of nanoparticles with a self-referenced and self-heterodyned whispering-gallery Raman microlaser. Proc. Natl. Acad. Sci. U S A *111*, E3836–E3844.

48. Chen, W., Özdemir, Ş.K., Zhao, G., Wiersig, J., and Yang, L. (2017). Exceptional points enhance sensing in an optical microcavity. Nature *548*, 192–196.

49. Wang, C., Jiang, X., Zhao, G., Zhang, M., Hsu, C.W., Peng, B., Stone, A.D., Jiang, L., and Yang, L. (2020). Electromagnetically induced transparency at a chiral exceptional point. Nat. Phys. *16*, 334–340.

50. Miri, M.A., and Alù, A. (2019). Exceptional points in optics and photonics. Science *363*, eaar7709.

51. Wiersig, J. (2014). Enhancing the sensitivity of frequency and energy splitting detection by using exceptional points: application to microcavity sensors for single-particle detection. Phys. Rev. Lett. *112*, 1–5.

52. Wiersig, J. (2016). Sensors operating at exceptional points: general theory. Phys. Rev. A *93*, 033809.

53. Li, B.B., Xiao, Y.F., Zou, C.L., Liu, Y.C., Jiang, X.F., Chen, Y.L., Li, Y., and Gong, Q. (2011). Experimental observation of Fano resonance in a single whispering-gallery microresonator. Appl. Phys. Lett. *98*, 021116.

54. Li, B.B., Xiao, Y.F., Zou, C.L., Jiang, X.F., Liu, Y.C., Sun, F.W., Li, Y., and Gong, Q. (2012). Experimental controlling of Fano resonance in indirectly coupled whispering-gallery microresonators. Appl. Phys. Lett. *100*, 021108.

55. Jiang, X., and Yang, L. (2020). Optothermal dynamics in whispering-gallery microresonators. Light Sci. Appl. *9*, 24.

56. Grudinin, I., Lee, H., Chen, T., and Vahala, K. (2011). Compensation of thermal nonlinearity effect in optical resonators. Opt. Express *19*, 7365.

57. He, L., Xiao, Y.F., Dong, C., Zhu, J., Gaddam, V., and Yang, L. (2008). Compensation of thermal refraction effect in high- Q toroidal microresonator by polydimethylsiloxane coating. Appl. Phys. Lett. *93*, 201102.

58. Suter, J.D., White, I.M., Zhu, H., and Fan, X. (2007). Thermal characterization of liquid core optical ring resonator sensors. Appl. Opt. *46*, 389–396.

59. Kim, E., Foreman, M.R., Baaske, M.D., and Vollmer, F. (2015). Thermal characterisation of (bio)polymers with a temperature-stabilised whispering gallery mode microsensor. Appl. Phys. Lett. *106*, 161101.

60. Fescenko, I., Alnis, J., Schliesser, A., Wang, C.Y., Kippenberg, T.J., and Hansch, T.W. (2012). Dual-mode temperature compensation technique for laser stabilization to a crystalline whispering gallery mode resonator. Opt. Express *20*, 19185–19193.

61. Le, T., Savchenkov, A., Yu, N., Maleki, L., and Steier, W.H. (2009). Optical resonant sensors: a method to reduce the effect of thermal drift. Appl. Opt. *48*, 458–463.

62. Hu, D., Zou, C.L., Ren, H., Lu, J., Le, Z., Qin, Y., Guo, S., Dong, C., and Hu, W. (2020). Multi-parameter sensing in a multimode self-interference micro-ring resonator by machine learning. Sensors *20*, 709.

63. Mallik, A.K., Farrell, G., Ramakrishnan, M., Kavungal, V., Liu, D., Wu, Q., and Semenova, Y. (2018). Whispering gallery mode micro resonators for multi-parameter sensing applications. Opt. Express *26*, 31829.

64. Chen, Z., Li, M., Wu, X., Liu, L., and Xu, L. (2015). 2-D optical/opto-mechanical microfluidic sensing with micro-bubble resonators. Opt. Express *23*, 17659.

65. Sun, Y., Shopova, S.I., Frye-Mason, G., and Fan, X. (2008). Rapid chemical-vapor sensing using optofluidic ring resonators. Opt. Lett. *33*, 788–790.

66. Park, M.K., Kee, J.S., Quah, J.Y., Netto, V., Song, J., Fang, Q., La Fosse, E.M., and Lo, G.Q. (2013). Label-free aptamer sensor based on silicon microring resonators. Sensors Actuators B Chem. *176*, 552–559.

67. Kim, E., Baaske, M.D., Schuldes, I., Wilsch, P.S., and Vollmer, F. (2017). Label-free optical detection of single enzyme-reactant reactions and associated conformational changes. Sci. Adv. *3*, e1603044.

68. Gavartin, E., Verlot, P., and Kippenberg, T.J. (2012). A hybrid on-chip optomechanical transducer for ultrasensitive force measurements. Nat. Nanotechnol. *7*, 509–514.

69. Li, B.-B., Bulla, D., Prakash, V., Forstner, S., Dehghan-Manshadi, A., Rubinsztein-Dunlop, H., Foster, S., and Bowen, W.P. (2018). On-chip scalable optomechanical magnetometers *1*, 1–6.

70. Ioppolo, T., Ayaz, U., and Otugen, M.V.((2009). Tuning of whispering gallery modes of spherical resonators using an external electric field. Opt. Express *17*, 16465–16479.

71. Madugani, R., Yang, Y., Le, V.H., Ward, J.M., and Nic Chormaic, S. (2016). Linear laser tuning using a pressure-sensitive microbubble resonator. IEEE Photon. Technol. Lett. *28*, 1134–1137.

72. Kim, K.H., Luo, W., Zhang, C., Tian, C., Jay Guo, L., Wang, X., and Fan, X. (2017). Air-coupled ultrasound detection using capillary-based optical ring resonators. Sci. Rep. *7*.

73. Ward, J.M., Yang, Y., and Chormaic, S.N. (2016). Flow sensor using a hollow whispering gallery mode microlaser. In: Proceedings of SPIE LASE.doi:10.1117/12.2209205.

74. Zhi, Y., Yu, X.-C., Gong, Q., Yang, L., and Xiao, Y.-F. (2017). Single nanoparticle detection using optical microcavities. Adv. Mater. *29*, 1604920.

75. Yu, X.C., Li, B.B., Wang, P., Tong, L., Jiang, X.F., Li, Y., Gong, Q., and Xiao, Y.F. (2014). Single nanoparticle detection and sizing using a nanofiber pair in an aqueous environment. Adv. Mater. *26*, 7462–7467.

76. Tang, S.J., Liu, S., Yu, X.C., Song, Q., Gong, Q., and Xiao, Y.F. (2018). On-chip spiral waveguides for ultrasensitive and rapid detection of nanoscale objects. Adv. Mater. *30*, 1800262.

77. Yu, X.C., Zhi, Y., Tang, S.J., Li, B.B., Gong, Q., Qiu, C.W., and Xiao, Y.F. (2018). Optically sizing single atmospheric particulates with a 10-nm resolution using a strong evanescent field. Light Sci. Appl. *7*, 18003.

78. Dantham, V.R., Holler, S., Kolchenko, V., Wan, Z., and Arnold, S. (2012). Taking whispering gallery-mode single virus detection and sizing to the limit. Appl. Phys. Lett. *101*, 043704.

79. Knapper, K.A., Heylman, K.D., Horak, E.H., and Goldsmith, R.H. (2016). Chip-scale fabrication of high-Q all-glass toroidal microresonators for single-particle label-free imaging. Adv. Mater. *28*, 2945–2950.

80. Heylman, K.D., Thakkar, N., Horak, E.H., Quillin, S.C., Cherqui, C., Knapper, K.A., Masiello, D.J., and Goldsmith, R.H. (2016). Optical microresonators as single-particle absorption spectrometers. Nat. Photonics *10*, 788–795.

81. Hogan, L.T., Horak, E.H., Ward, J.M., Knapper, K.A., Nic Chormaic, S., and Goldsmith, R.H. (2019). Toward real-time monitoring and control of single nanoparticle properties with a microbubble resonator spectrometer. ACS Nano *13*, 12743–12757.

82. Horak, E.H., Rea, M.T., Heylman, K.D., Gelbwaser-Klimovsky, D., Saikin, S.K., Thompson, B.J., Kohler, D.D., Knapper, K.A., Wei, W., Pan, F., et al. (2018). Exploring electronic structure and order in polymers via single-particle microresonator spectroscopy. Nano Lett. *18*, 1600–1607.

83. Suh, J., Han, K., and Bahl, G. (2018). Imaging of acoustic pressure modes in opto-mechano-fluidic resonators with a single particle probe. Appl. Phys. Lett. *112*.

84. Ward, J.M., Yang, Y., Lei, F., Yu, X.-C., Xiao, Y.-F., and Chormaic, S.N. (2018). Nanoparticle sensing beyond evanescent field interaction with a quasi-droplet microcavity. Optica *5*, 674–677.

85. Wildgen, S.M., and Dunn, R.C. (2015). Whispering gallery mode resonators for rapid label-free biosensing in small volume droplets. Biosensors *5*, 118–130.

86. Washburn, A.L., Luchansky, M.S., Bowman, A.L., and Bailey, R.C. (2010). Quantitative, label-free detection of five protein biomarkers using multiplexed arrays of silicon photonic microring resonators. Anal. Chem. *82*, 69–72.

87. Luchansky, M.S., Washburn, A.L., McClellan, M.S., and Bailey, R.C. (2011). Sensitive on-chip detection of a protein biomarker in human serum and plasma over an extended dynamic range using silicon photonic microring resonators and sub-micron beads. Lab Chip *11*, 2042.

88. Kindt, J.T., Luchansky, M.S., Qavi, A.J., Lee, S.-H., and Bailey, R.C. (2013). Subpicogram per milliliter detection of interleukins using silicon photonic microring resonators and an enzymatic signal enhancement strategy. Anal. Chem. *85*, 10653–10657.

89. Valera, E., McClellan, M.S., and Bailey, R.C. (2015). Magnetically-actuated, bead-enhanced silicon photonic immunosensor. Anal. Methods *7*, 8539–8544.

90. Qavi, A.J., Mysz, T.M., and Bailey, R.C. (2011). Isothermal discrimination of single-nucleotide polymorphisms via real-time kinetic desorption and label-free detection of DNA using silicon photonic microring resonator arrays. Anal. Chem. *83*, 6827–6833.

91. Suter, J.D., White, I.M., Zhu, H., Shi, H., Caldwell, C.W., and Fan, X. (2008). Label-free quantitative DNA detection using the liquid core optical ring resonator. Biosens. Bioelectron. *23*, 1003–1009.

92. Vollmer, F., Arnold, S., Braun, D., Teraoka, I., and Libchaber, A. (2003). Multiplexed DNA quantification by spectroscopic shift of two microsphere cavities. Biophys. J. *85*, 1974–1979.

93. Qavi, A.J., Kindt, J.T., Gleeson, M.A., and Bailey, R.C. (2011). Anti-DNA:RNA antibodies and silicon photonic microring resonators: increased sensitivity for multiplexed

microRNA detection. Anal. Chem. *83*, 5949–5956.

94. Graybill, R.M., Para, C.S., and Bailey, R.C. (2016). PCR-free, multiplexed expression profiling of microRNAs using silicon photonic microring resonators. Anal. Chem. *88*, 10347–10351.

95. Anderson, M.E., O'Brien, E.C., Grayek, E.N., Hermansen, J.K., and Hunt, H.K. (2015). The detection of helicobacter hepaticus using whispering-gallery mode microcavity optical sensors. Biosensors *5*, 562–576.

96. Ghali, H., Bianucci, P., and Peter, Y.A. (2017). Wavelength shift in a whispering gallery microdisk due to bacterial sensing: a theoretical approach. Sens. Bio. Sens. Res. *13*, 9–16.

97. Ghali, H., Chibli, H., Nadeau, J.L., Bianucci, P., and Peter, Y.A. (2016). Real-time detection of Staphylococcus aureus using Whispering Gallery Mode optical microdisks. Biosensors *6*, 20.

98. Gohring, J.T., and Fan, X. (2010). Label free detection of $CD4^+$ and $CD8^+$ T cells using the optofluidic ring resonator. Sensors *10*, 5798–5808.

99. McClellan, M.S., Domier, L.L., and Bailey, R.C. (2012). Label-free virus detection using silicon photonic microring resonators. Biosens. Bioelectron. *31*, 388–392.

100. Lu, T., Lee, H., Chen, T., Herchak, S., Kim, J.-H., Fraser, S.E., Flagan, R.C., and Vahala, K. (2011). High sensitivity nanoparticle detection using optical microcavities. Proc. Natl. Acad. Sci. U S A *108*, 5976–5979.

101. Washburn, A.L., Shia, W.W., Lenkeit, K.A., Lee, S.H., and Bailey, R.C. (2016). Multiplexed cancer biomarker detection using chip-integrated silicon photonic sensor arrays. Analyst *141*, 5358–5365.

102. Sloan, C.D.K., Marty, M.T., Sligar, S.G., and Bailey, R.C. (2013). Interfacing lipid bilayer nanodiscs and silicon photonic sensor arrays for multiplexed protein-lipid and protein-membrane protein interaction screening. Anal. Chem. *85*, 2970–2976.

103. Muehl, E.M., Gajsiewicz, J.M., Medfisch, S.M., Wiersma, Z.S.B., Morrissey, J.H., and Bailey, R.C. (2017). Multiplexed silicon photonic sensor arrays enable facile characterization of coagulation protein binding to nanodiscs with variable lipid content. J. Biol. Chem. 16249–16256.

104. Basiri-Esfahani, S., Armin, A., Forstner, S., and Bowen, W.P. (2019). Precision ultrasound sensing on a chip. Nat. Commun. *10*.

105. Xu, X., Jiang, X., Zhao, G., and Yang, L. (2016). Phone-sized whispering-gallery microresonator sensing system. Opt. Express *24*, 25905.

106. Passaro, M.V., Dell'Olio, F., and De Leonardis, F. (2007). Ammonia optical sensing by microring resonators. Sensors *7*, 2741–2749.

107. Sun, Y., Liu, J., Frye-Mason, G., Ja, S., Thompson, A.K., and Fan, X. (2009). Optofluidic ring resonator sensors for rapid DNT vapor detection. Analyst *134*, 1386–1391.

108. Gregor, M., Pyrlik, C., Henze, R., Wicht, A., Peters, A., and Benson, O. (2010). An alignment-free fiber-coupled microsphere resonator for gas sensing applications. Appl. Phys. Lett. *96*, 231102.

109. Yao, B., Yu, C., Wu, Y., Huang, S.W., Wu, H., Gong, Y., Chen, Y., Li, Y., Wong, C.W., Fan, X., et al. (2017). Graphene-enhanced brillouin optomechanical microresonator for ultrasensitive gas detection. Nano Lett. *17*, 4996–5002.

110. Nam, S.H., and Yin, S. (2005). High-temperature sensing using whispering gallery mode resonance in bent optical fibers. IEEE Photon. Technol. Lett. *17*, 2391–2393.

111. Guan, G., Arnold, S., and Otugen, V. (2006). Temperature measurements using a microoptical sensor based on whispering gallery modes. AIAA J. *44*, 2385–2389.

112. Guha, B., Cardenas, J., and Lipson, M. (2013). Athermal silicon microring resonators with titanium oxide cladding. Opt. Express *21*, 26557.

113. Dong, C.-H., He, L., Xiao, Y.-F., Gaddam, V.R., Ozdemir, S.K., Han, Z.-F., Guo, G.-C., and Yang, L. (2009). Fabrication of high- Q polydimethylsiloxane optical microspheres for thermal sensing. Appl. Phys. Lett. *94*.

114. Li, B.-B., Wang, Q.-Y., Xiao, Y.-F., Jiang, X.-F., Li, Y., Xiao, L., and Gong, Q. (2010). On chip, high-sensitivity thermal sensor based on high-Q polydimethylsiloxane-coated microresonator. Appl. Phys. Lett. *96*, 251109.

115. Yan, Y.-Z., Zou, C.-L., Yan, S.-B., Sun, F.-W., Ji, Z., Liu, J., Zhang, Y.-G., Wang, L., Xue, C.-Y., Zhang, W.-D., et al. (2011). Packaged silica microsphere-taper coupling system for robust thermal sensing application. Opt. Express *19*, 5753.

116. Luo, R., Jiang, H., Liang, H., Chen, Y., and Lin, Q. (2017). Self-referenced temperature sensing with a lithium niobate microdisk resonator. Opt. Lett. *42*, 1281–1284.

117. Ioppolo, T., and Manzo, M. (2014). Dome-shaped whispering gallery mode laser for remote wall temperature sensing. Appl. Opt. *53*, 5065–5069.

118. Liu, Y., Jiang, X., Wang, C., and Yang, L. (2020). Optothermally induced mechanical oscillation in a silk fibroin coated high- Q microsphere. Appl. Phys. Lett. *116*, 201104.

119. Zhu, S., Shi, L., Liu, N., Xu, X., and Zhang, X. (2017). Magnetic field sensing using magnetic-fluid-filled optofluidic ring resonator. Microfluid. Nanofluidics *21*, 156.

120. Zhu, J., Zhao, G., Savukov, I., and Yang, L. (2017). Polymer encapsulated microcavity optomechanical magnetometer. Sci. Rep. *7*, 8896.

121. Manzo, M., Ioppolo, T., Ayaz, U.K., Lapenna, V., and Ötügen, M.V. (2012). A photonic wall pressure sensor for fluid mechanics applications. Rev. Sci. Instrum. *83*.

122. Yang, Y., Saurabh, S., Ward, J.M., and Nic Chormaic, S. (2016). High-Q, ultrathin-walled microbubble resonator for aerostatic pressure sensing. Opt. Express *24*, 294.

123. Hanumegowda, N.M., Stica, C.J., Patel, B.C., White, I., and Fan, X. (2005). Refractometric sensors based on microsphere resonators. Appl. Phys. Lett. *87*.

124. Huang, S.H.S.H., Sheth, S., Jain, E., Jiang, X., Zustiak, S.P.S.P., and Yang, L. (2018). Whispering gallery mode resonator sensor for in situ measurements of hydrogel gelation. Opt. Express *26*, 51.

125. Yang, D., Wang, A., Chen, J., Yu, X.-C., Lan, C., Ji, Y., and Xiao, Y.-F. (2020). Real-time monitoring of hydrogel phase transition in an ultrahigh Q microbubble resonator. Photonics Res. *8*, 497–502.

126. Passaro, V.M.N., and De Leonardis, F. (2006). Modeling and design of a novel high-sensitivity electric field silicon-on-insulator sensor based on a whispering-gallery-mode resonator. IEEE J. Sel. Top. Quan. Electron. *12*, 126–133.

127. Armani, D., Min, B., Martin, A., and Vahala, K.J. (2004). Electrical thermo-optic tuning of ultrahigh-Q microtoroid resonators. Appl. Phys. Lett. *85*, 5439–5441.

128. Bhola, B., Nosovitskiy, P., Mahalingam, H., and Steier, W.H. (2009). Sol-gel-based integrated optical microring resonator humidity sensor. IEEE Sens. J. *9*, 740–747.

129. Mehrabani, S., Kwong, P., Gupta, M., and Armani, A.M. (2013). Hybrid microcavity humidity sensor. Appl. Phys. Lett. *102*.

130. Matsko, A., Savchenkov, A., Ilchenko, V., and Maleki, L. (2004). Optical gyroscope with whispering gallery mode optical cavities. Opt. Commun. *233*, 107–112.

131. Li, J., Suh, M.-G., and Vahala, K. (2017). Microresonator brillouin gyroscope. Optica *4*, 346.

132. Trocha, P., Karpov, M., Ganin, D., Pfeiffer, M.H.P., Kordts, A., Wolf, S., Krockenberger, J., Marin-Palomo, P., Weimann, C., Randel, S., et al. (2018). Ultrafast optical ranging using microresonator soliton frequency combs. Science *359*, 887.

133. Suh, M.G., and Vahala, K.J. (2018). Soliton microcomb range measurement. Science *359*, 884.

134. Suh, M.G., Yi, X., Lai, Y.H., Leifer, S., Grudinin, I.S., Vasisht, G., Martin, E.C., Fitzgerald, M.P., Doppmann, G., Wang, J., et al. (2019). Searching for exoplanets using a microresonator astrocomb. Nat. Photonics *13*, 25–30.

135. Barnard, A.W., Zhang, M., Wiederhecker, G.S., Lipson, M., and McEuen, P.L. (2019). Real-time vibrations of a carbon nanotube. Nature *566*, 89.

136. Jiang, X., Shao, L., Zhang, S.X., Yi, X., Wiersig, J., Wang, L., Gong, Q., Loncar, M., Yang, L., and Xiao, Y.F. (2017). Chaos-assisted broadband momentum transformation in optical microresonators. Science *358*, 344–347.

137. Jiang, X.F., Zou, C.L., Wang, L., Gong, Q., and Xiao, Y.F. (2016). Whispering-gallery microcavities with unidirectional laser emission. Laser Photon. Rev. *10*, 40–61.

138. Jiang, X.F., Xiao, Y.F., Zou, C.L., He, L., Dong, C.H., Li, B.B., Li, Y., Sun, F.W., Yang, L., and Gong, Q. (2012). Highly unidirectional emission and ultralow-threshold lasing from on-chip ultrahigh-Q microcavities. Adv. Mater. *24*, OP260–OP264.

139. Liu, Z.P., Jiang, X.F., Li, Y., Xiao, Y.F., Wang, L., Ren, J.L., Zhang, S.J., Yang, H., and Gong, Q. (2013). High-Q asymmetric polymer microcavities directly fabricated by two-photon polymerization. Appl. Phys. Lett. *102*, 221108.

140. Shao, L., Wang, L., Xiong, W., Jiang, X.F., Yang, Q.F., and Xiao, Y.F. (2013). Ultrahigh-Q, largely deformed microcavities coupled by a free-space laser beam. Appl. Phys. Lett. *103*.

141. Wang, L., Lippolis, D., Li, Z.Y., Jiang, X.F., Gong, Q., and Xiao, Y.F. (2016). Statistics of chaotic resonances in an optical microcavity. Phys. Rev. E *93*, 040201.

142. Xiao, Y.F., Jiang, X.F., Yang, Q.F., Wang, L., Shi, K., Li, Y., and Gong, Q. (2013). Tunneling-induced transparency in a chaotic microcavity. Laser Photon. Rev. *7*, L51–L54.

143. Kullig, J., Jiang, X., Yang, L., and Wiersig, J. (2020). Microstar cavities: an alternative concept for the confinement of light. Phys. Rev. Res. *2*, 012072.

144. Lei, F., Tkachenko, G., Jiang, X., Ward, J.M., Yang, L., and Chormaic, S.N. (2020). Enhanced directional coupling of light with a whispering gallery microcavity. ACS Photonics *7*, 361.

145. Shu, F., Jiang, X., Zhao, G., and Yang, L. (2018). A scatterer-assisted whispering-gallery-mode microprobe. Nanophotonics *7*, 1455–1460.

146. Liu, Y.C., Xiao, Y.F., Jiang, X.F., Li, B.B., Li, Y., and Gong, Q. (2012). Cavity-QED treatment of scattering-induced free-space excitation and collection in high-Q whispering-gallery microcavities. Phys. Rev. A Mol. Opt. Phys. *85*, 013843.

147. Tang, S.J., Liu, Z., Qian, Y.J., Shi, K., Sun, Y., Wu, C., Gong, Q., and Xiao, Y.F. (2018). A tunable optofluidic microlaser in a photostable conjugated polymer. Adv. Mater. *30*, 1804556.

148. Wan, S., Niu, R., Ren, H.-L., Zou, C.-L., Guo, G.-C., and Dong, C.-H. (2018). Experimental demonstration of dissipative sensing in a self-interference microring resonator. Photonics Res. *6*, 681–685.

149. Ren, H., Zou, C.-L., Lu, J., Le, Z., Qin, Y., Guo, S., and Hu, W. (2019). Dissipative sensing with low detection limit in a self-interference microring resonator. J. Opt. Soc. Am. B *36*, 942.

150. Ren, H., Zou, C.L., Lu, J., Xue, L.L., Guo, S., Qin, Y., and Hu, W. (2016). Highly sensitive intensity detection by a self-interference micro-ring resonator. IEEE Photonics Technol. Lett. *28*, 1469.

151. Xu Xiangyi, Chen Weijian, Zhao Guangming, Li Yihang, Lu Chenyang, and Yang Lan (2018). Wireless whispering-gallery-mode sensor for thermal sensing and aerial mapping. Light: science & applications *7*, 62.